Towards Accurate DeepMD Potentials for Aqueous Interfaces

Christian Loer Llemit

August 2024

Contents

Chapter 1

Introduction

Chapter 2

Methodology

Initial trajectories were generated using Molecular Dynamics implemented in LAMMPS [1]. The pair potential used is based on the previously trained deep neural network potential (NNP) conducted by Sanchez-Burgos et al. [2].

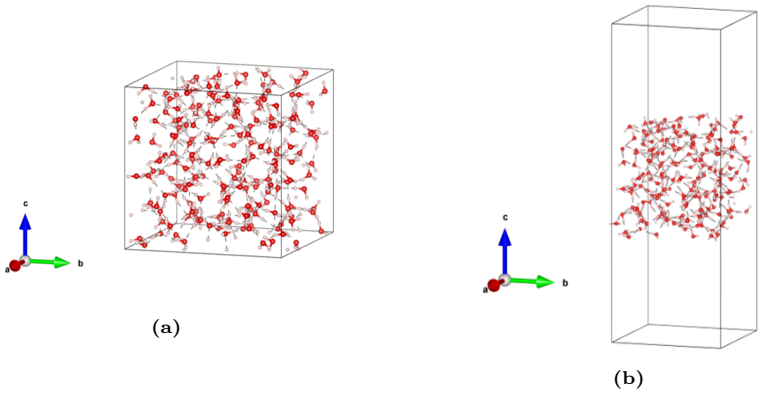

Fig. 2.1: Typical configurations for (a) bulk and (b) slab systems.

For the MD simulation, a system size of 192 water molecules was used for both the bulk and slab systems, as shown in Figure 2.1. The temperature was varied from 300 K to 600 K. The simulation profile of the bulk system is as follows: NPT ensemble at 1 bar for 2 ns, and a ramp from 1 bar to 10,000 bar for 10 ns. For the slab system, the simulation was done in NVT ensemble for 10 ns and the box size was based on the average length of the corresponding bulk system at a given temperature and at 1 bar. Vacuum was introduced as to create a total length of 50 Å in the direction normal to the interface. For both systems, a simulation step of 0.2 fs, thermostat relaxation time of 20 fs, and barostat relaxation time of 200 fs were applied. The surface tension was calculated according to Kirkwood-Buff equation [3] given by

$$\gamma = \frac{L_z}{2}\left[\langle P_{zz}\rangle - \frac{1}{2}\left(\langle P_{xx}\rangle + \langle P_{yy}\rangle\right)\right] \tag{2.1}$$

The trajectories were then labeled with their energy, force, and pressure tensor using Density Functional Theory (DFT) implemented in Quantum Espresso [4–6]. Strongly Constrained and Appropriately Normed (SCAN) exchange-correlation functional is widely used in the study of water systems due to its great predictability in describing hydrogen bonds and van der Waals interac-

tions [7, 8]. However, for this study, the SCAN functional tends to be not numerically robust when implemented to systems with interfaces. Instead, this study tried to use accurate and numerically efficient r^{2}SCAN meta-generalized gradient approximation [9]. Optimized Norm-Conserving Vanderbilt pseudopotentials [10] were used with energy cutoff of 130 Ry and scf convergence threshold of 1×10^{-6} Ry.

The labeled frames were then feed into DeePMD-kit code [11–14] for the training of deep neural network potentials. A total of 7120 bulk frames and 2160 interface frames were used as training data. The training follows a typical two-neutral network architecture. First, atomic configurations are processed by the embedding network of three layers consisting of 25, 50 and 100 neurons each. The embedding follows the two-body smooth-edition scheme [15] that conserves radial and angular information within the cutoff radius of 6 Å. A switching function was applied for atoms beyond 5.5 Å to ensure smooth cutoff. Then, the atomic descriptors are build and given as input to a fitting network of three layers of 250 neurons each that outputs a scalar quantity such as energy. The parameters of the neural networks are set during the training procedure by minimizing loss function based on the mean squared error on the total energy and atomic forces predicted by the network with respect to the reference data. The iterative minimization was performed with a total of 4 million batches and a learning rate that exponentially decay from 1×10^{-3} to 3.51×10^{-8}.

Chapter 3

Theory

Chapter 4

Results and Discussion

4.1 Convergence Tests

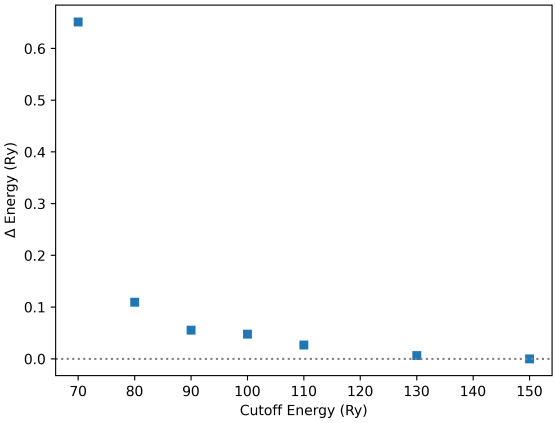

Fig. 4.1: Convergence in Energy

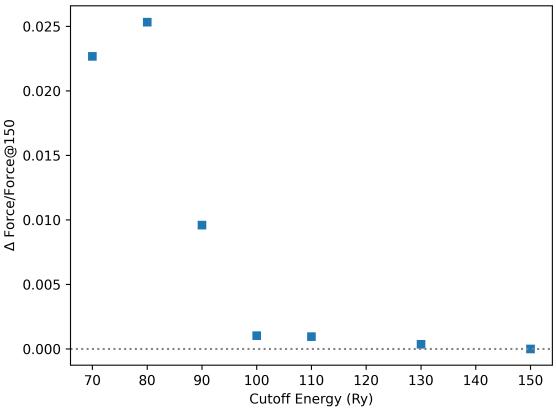

Fig. 4.2: Convergence in Force

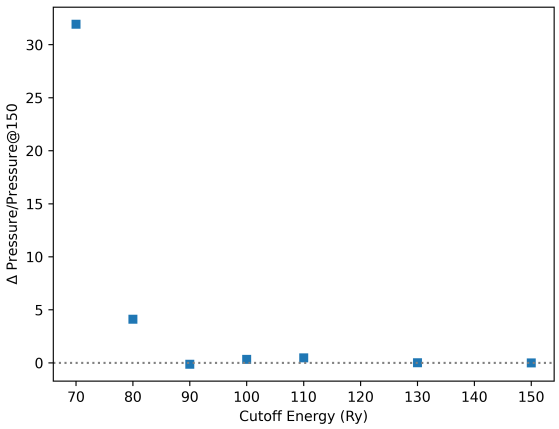

Fig. 4.3: Convergence in Pressure

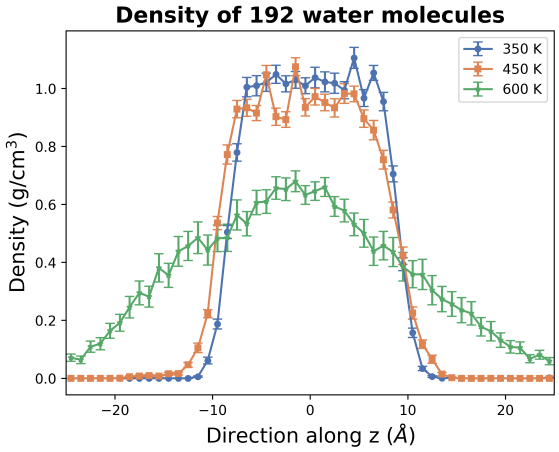

Fig. 4.4: Mass Density Profile for different temperature.

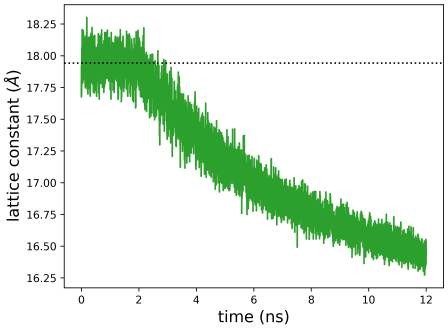

Fig. 4.5: Lattice parameter as a function of simulation steps.

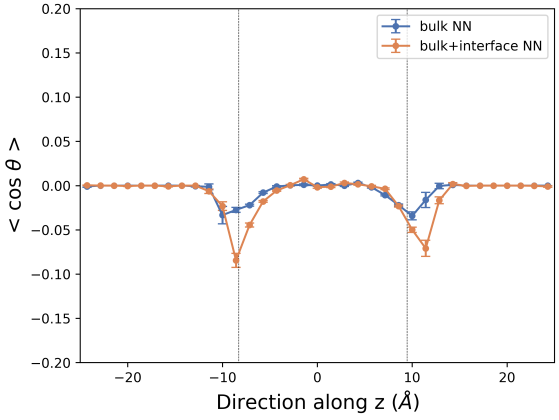

Fig. 4.6: Dipole Orientation

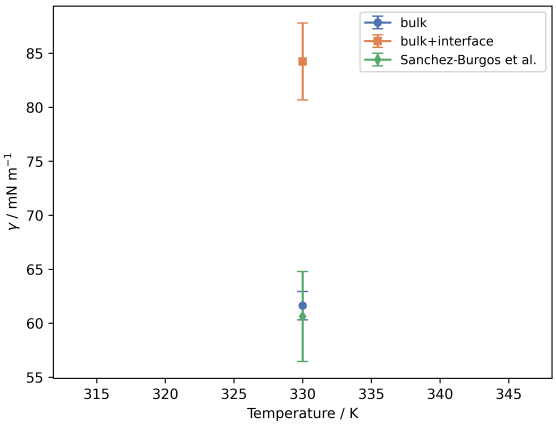

Fig. 4.7: Surface Tension

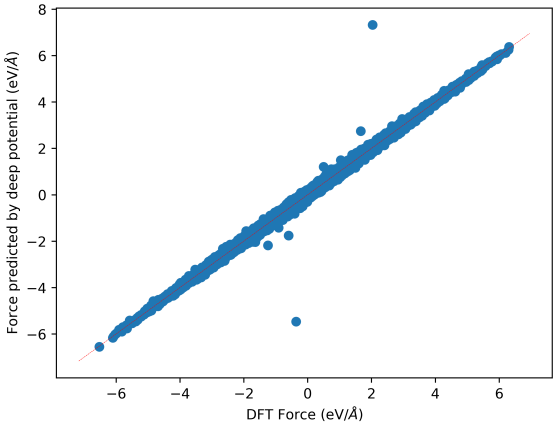

Fig. 4.8: Correlation between the predicted and reference data

4.2 SCAN vs. r2SCAN

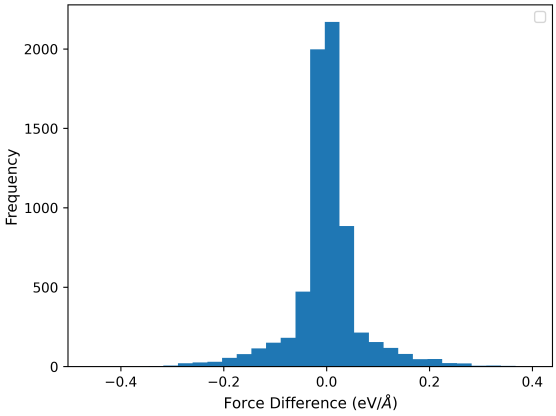

Fig. 4.9: Distribution of the Difference between SCAN and r2SCAN functional.

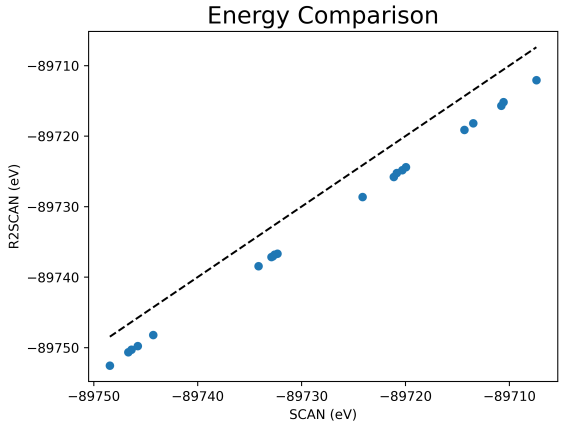

Fig. 4.10: Correlation of energy between SCAN and r2SCAN functional.

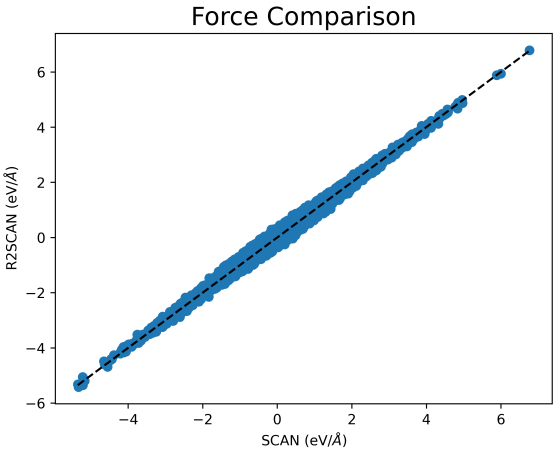

Fig. 4.11: Correlation of forces between SCAN and r2SCAN functional.

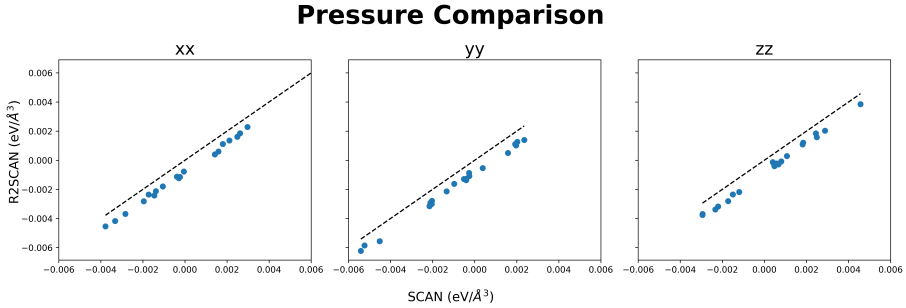

Fig. 4.12: Correlation of pressure between SCAN and r2SCAN functional.

Bibliography

[1] A. P. Thompson *et al.*, "LAMMPS - a flexible simulation tool for particle-based materials modeling at the atomic, meso, and continuum scales," *Comp. Phys. Comm.*, vol. 271, p. 108 171, 2022. DOI: 10.1016/j.cpc.2021.108171.

[2] I. Sanchez-Burgos, M. C. Muniz, J. R. Espinosa, and A. Z. Panagiotopoulos, "A deep potential model for liquid–vapor equilibrium and cavitation rates of water," *The Journal of Chemical Physics*, vol. 158, no. 18, 2023.

[3] J. G. Kirkwood and F. P. Buff, "The statistical mechanical theory of surface tension," *The Journal of Chemical Physics*, vol. 17, no. 3, pp. 338–343, 1949.

[4] P. Giannozzi *et al.*, "Quantum espresso: A modular and open-source software project for quantum simulations of materials," *Journal of Physics: Condensed Matter*, vol. 21, no. 39, 395502 (19pp), 2009.

[5] P. Giannozzi *et al.*, "Advanced capabilities for materials modelling with quantum espresso," *Journal of Physics: Condensed Matter*, vol. 29, no. 46, p. 465 901, 2017.

[6] P. Giannozzi *et al.*, "Quantum espresso toward the exascale," *The Journal of Chemical Physics*, vol. 152, no. 15, p. 154 105, 2020. DOI: 10.1063/5.0005082.

[7] J. Sun, A. Ruzsinszky, and J. P. Perdew, "Strongly constrained and appropriately normed semilocal density functional," *Physical review letters*, vol. 115, no. 3, p. 036 402, 2015.

[8] M. Chen *et al.*, "Ab initio theory and modeling of water," *Proceedings of the National Academy of Sciences*, vol. 114, no. 41, pp. 10 846–10 851, 2017.

[9] J. W. Furness, A. D. Kaplan, J. Ning, J. P. Perdew, and J. Sun, "Accurate and numerically efficient r2scan meta-generalized gradient approximation," *The Journal of Physical Chemistry Letters*, vol. 11, no. 19, pp. 8208–8215, 2020, PMID: 32876454. DOI: 10.1021/acs.jpclett.0c02405.

[10] D. Hamann, "Optimized norm-conserving vanderbilt pseudopotentials," *Physical Review B—Condensed Matter and Materials Physics*, vol. 88, no. 8, p. 085 117, 2013.

[11] H. Wang, L. Zhang, J. Han, and E. Weinan, "Deepmd-kit: A deep learning package for many-body potential energy representation and molecular dynamics," *Computer Physics Communications*, vol. 228, pp. 178–184, 2018.

[12] J. Zeng *et al.*, "Deepmd-kit v2: A software package for deep potential models," *The Journal of Chemical Physics*, vol. 159, no. 5, 2023.

[13] D. Lu *et al.*, "86 pflops deep potential molecular dynamics simulation of 100 million atoms with ab initio accuracy," *Computer Physics Communications*, vol. 259, p. 107 624, 2021.

[14] L. Zhang, J. Han, H. Wang, W. Saidi, R. Car, *et al.*, "End-to-end symmetry preserving inter-atomic potential energy model for finite and extended systems," *Advances in neural information processing systems*, vol. 31, 2018.

[15] L. Zhang, J. Han, H. Wang, W. Saidi, R. Car, and W. E, "End-to-end symmetry preserving inter-atomic potential energy model for finite and extended systems," in *Advances in Neural Information Processing Systems*, S. Bengio, H. Wallach, H. Larochelle, K. Grauman, N. Cesa-Bianchi, and R. Garnett, Eds., vol. 31, Curran Associates, Inc., 2018. [Online]. Available: `https://proceedings.neurips.cc/paper_files/paper/2018/file/e2ad76f2326fbc6b56a45a56c59fafdb-Paper.pdf`.